Deep-Sea Research I 108 (2016) 58–72

Contents lists available at ScienceDirect

Deep-Sea Research I

journal homepage: www.elsevier.com/locate/dsri

Regional- and local-scale variations in benthic megafaunal composition at the Arctic deep-sea observatory HAUSGARTEN

J. Taylor*, T. Krumpen, T. Soltwedel, J. Gutt, M. Bergmann

Alfred-Wegener-Institut, Helmholtz-Zentrum für Polar- und Meeresforschung, Am Handelshafen 12, D-27570 Bremerhaven, Germany

ARTICLE INFO

Article history:
Received 16 June 2015
Received in revised form
18 December 2015
Accepted 21 December 2015
Available online 22 December 2015

Keywords:
Arctic
Deep sea
Image analysis
Epibenthic megafauna
Observatory
Photo/video system
Scale
Species turnover

ABSTRACT

The Long-Term Ecological Research (LTER) observatory HAUSGARTEN, in the eastern Fram Strait, provides us the valuable ability to study the composition of benthic megafaunal communities through the analysis of seafloor photographs. This, in combination with extensive sampling campaigns, which have yielded a unique data set on faunal, bacterial, biogeochemical and geological properties, as well as on hydrography and sedimentation patterns, allows us to address the question of why variations in megafaunal community structure and species distribution exist within regional (60–110 km) and local (< 4 km) scales.

Here, we present first results from the latitudinal HAUSGARTEN gradient, consisting of three different stations (N3, HG-IV, S3) between 78°30′N and 79°45′N (2351–2788 m depth), obtained via the analysis of images acquired by a towed camera (OFOS-Ocean Floor Observation System) in 2011. We assess variability in megafaunal densities, species composition and diversity as well as biotic and biogenic habitat features, which may cause the patterns observed. While there were significant regional-scale differences in megafaunal composition and densities between the stations (N3 = 26.74 ± 0.63; HG-IV = 11.21 ± 0.25; S3 = 18.34 ± 0.39 individuals m^{-2}), significant local differences were only found at HG-IV.

Regional-scale variations may be due to the significant differences in ice coverage at each station as well as the different quantities of protein available, whereas local-scale differences at HG-IV may be a result of variation in bottom topography or factors not yet identified.

1. Introduction

Ecosystems deeper than 2000 m cover ~60% of the Earth's surface (Smith et al., 2009) and represent the world's most vast biome. Because of technological and time constraints, < 1% of this has been studied. Still less is known about these ecosystems in remote Polar Regions, as they are even less accessible due to ice cover and harsh environmental conditions for most of the year. This study focuses on the megabenthic composition of a polar, soft-sediment ecosystem.

Epibenthic megafauna inhabit the sediment-water interface and are traditionally described as those organisms that are visible in photographs and/or are > 1.5 cm (Grassle et al., 1975; Rex, 1981). With the continual development of camera definition, here we move towards the one definition of > 1.5 cm as many organisms smaller than that can now be identified with modern high-resolution cameras. Megabenthic organisms are physical developers of their surrounding landscape, with mobile megafauna creating tracks (in this study referred to as 'Lebensspuren'), burrows and mounds. This function has them performing as ecosystem engineers (Jones et al., 1994), increasing habitat heterogeneity, creating potential for greater diversity of smaller infauna (Soltwedel and Vopel, 2001; Quéric and Soltwedel, 2007). In their role as ecosystem engineers they are also involved in the continuous redistribution of organic matter, oxygen and nutritional matter in the surface sediments *via* bioturbation, oxygenation and remineralisation (Buhl-Mortensen et al., 2015). These processes are considered important in the global carbon cycle and further knowledge is needed to understand the key role they play in the world's largest carbon sink (Bett et al., 2001; Ruhl, 2007; Fitz-George-Balfour et al., 2010). Sessile megafauna can also play an integral role in a habitat by becoming structural keystones forming complex biogenic structures, and creating a further habitat niche that can provide the substratum needed for epibionts or attract mobile species that are in search of shelter or protection from predation (Buhl-Mortensen et al., 2010; Meyer et al., 2014).

While there have been previous studies on megafaunal composition at HAUSGARTEN with reference to: zonation patterns in both megafaunal abundances and community composition along a bathymetric gradient (Soltwedel et al., 2009), interannual changes between 2002 and 2007 at HG-IV and HG I (Bergmann et al., 2011;

* Corresponding author.
E-mail addresses: James.taylor@awi.de (J. Taylor), Thomas.krumpen@awi.de (T. Krumpen), Thomas.soltwedel@awi.de (T. Soltwedel), Julian.gutt@awi.de (J. Gutt), Melanie.bergmann@awi.de (M. Bergmann).

http://dx.doi.org/10.1016/j.dsr.2015.12.009

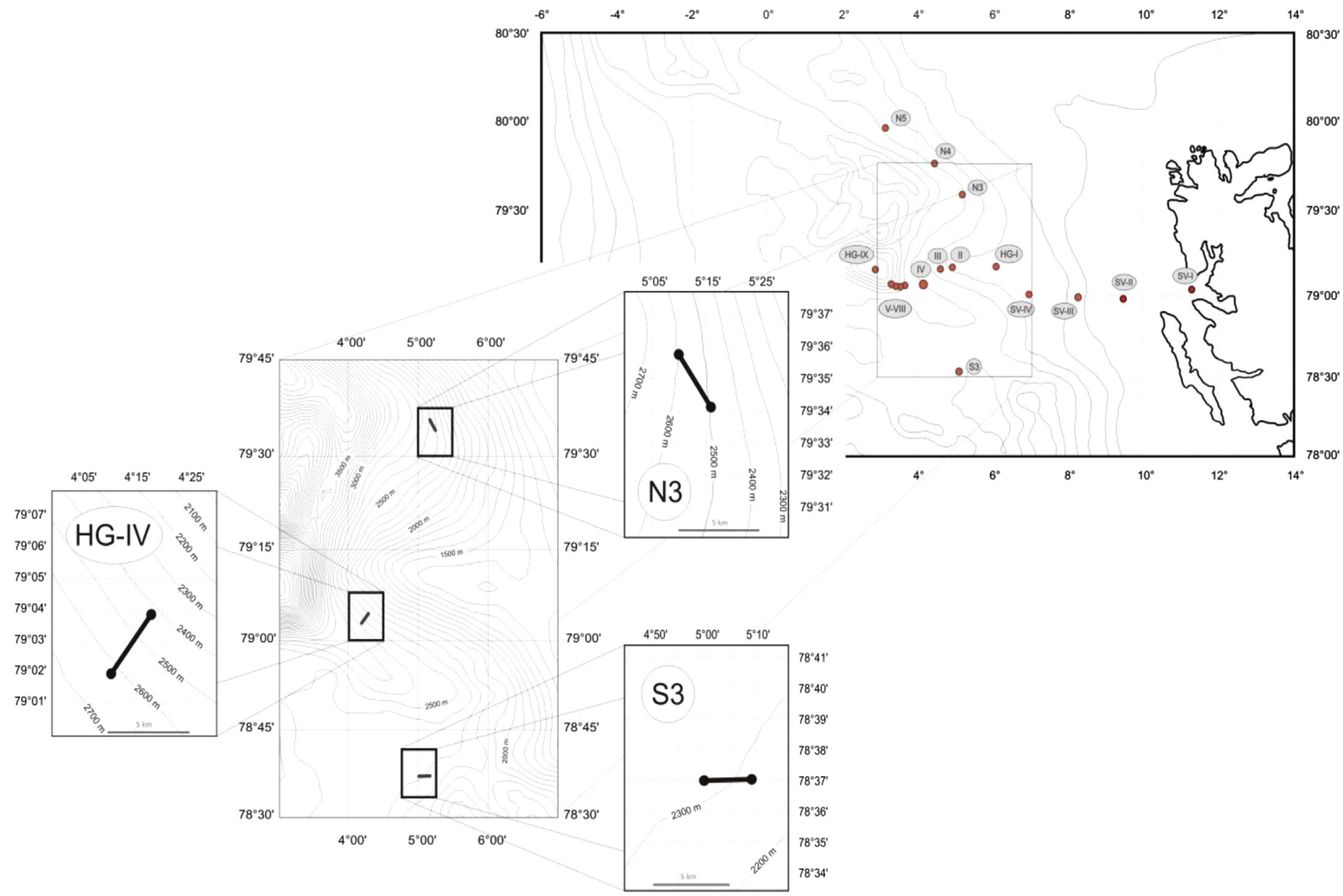

Fig. 1. Map of the LTER observatory HAUSGARTEN and the location of camera transects conducted at stations N3, HG-IV and S3.

Meyer et al., 2013) and zonation over a deep-water rocky reef (Meyer et al., 2014), this study provides the first assessment of regional-and local-scale spatial variations along a latitudinal gradient in the study area. This is also the first study to assess potential variations in α, β and γ diversity indices. The terms regional and local scale are often subjective in the literature, e.g. Whitman et al. (2004) has local scale at metres to hundreds of metres and regional scale at 200 to thousands of kilometres compared to Jacob et al. (2013) describing local to regional scale as 1–100 km, however, despite the specific distances given local scale is always described as a smaller sub-unit of regional scale. Here we describe regional variations as those between stations on a scale of 60–110 km whereas we consider local variations as those within a photographic transect, i.e. on a scale of <4 km ($\sim$2 nautical miles). Previous studies have largely focused on variations in species richness (Grassle and Maciolek, 1992; Whitman et al., 2004) with large-scale/regional latitudinal variations of species diversity amongst the deep-sea benthos, particularly of bivalves, gastropods and isopods (Rex et al., 1993), being observed. Knowledge of the spatial turnover of species becomes increasingly important in the design of marine protected areas and the issuance process of test-mining and exploitation permits for deep-sea mining (Wedding et al., 2013).

It is well documented that climate change is causing a retreat of polar ice and mountain glaciers. However, Arctic sea ice is declining at even greater rate than previously shown in model projections (Kauker et al., 2009), which leads to increased human pressure in the area from activities such as fishing, shipping and pollution (Bergmann and Klages, 2012; Sswat et al., 2015). Primary production may rise only slightly, if at all, as increased thermal or haline stratification will limit mixing and upward nutrient transport despite temperature and light penetration increasing because of the shrinking sea ice (e.g. Carmack and Wassmann, 2006). In addition, mesozooplankton abundance may increase in the Fram Strait if Atlantic species extend their range (Hirche and Kosobokova, 2007; Wassmann et al., 2010), which would amplify the high grazing pressure and lead to an increasingly retentive system (Forest et al., 2010). Consequently, the retreat of the ice edge and the continuous loss of multi-year ice may lead to a lower flux of fast-sinking ice algae and ice-related particulate organic matter (Gutt, 1995; Hop et al., 2006; Boetius et al., 2013). This could result in a decreased carbon deposition at the deep seafloor, which is already characterised by food limitation (Smith et al., 2008) and could finally alter benthic communities.

It was to address these issues and provide baselines that the Long-Term Ecological Research (LTER) observatory HAUSGARTEN (Soltwedel et al., 2005) was established, with the latitudinal transect set up specifically to study the influence of the marginal ice zone. Here, we assess regional and local-scale variations in the benthic megafaunal community by analysis of seafloor photographs from three stations along the latitudinal transect and by dividing each OFOS (Ocean Floor Observation System) transect into sub-sections. We address the following questions: (1) Do megafaunal density, composition and diversity differ between HAUSGARTEN stations along a latitudinal gradient? (2) Do megafaunal density, composition and diversity differ within a transect at a given station? We discuss these questions in terms of environmental parameters, sea–ice concentration and biogenic habitat features with an aim to interpret the observed variability.

2. Material and methods

2.1. Study location

Our study focused on three stations of the HAUSGARTEN observatory in the eastern Fram Strait, the only deep-water connection for the exchange of deep and intermediate water masses between the north Atlantic and true Arctic Ocean (Fahrbach et al., 2001). The hydrography in eastern parts of the strait is characterised by the inflow of relatively warm, nutrient-rich water into the central Arctic Ocean (Beszczynska-MÖller et al., 2012).

HAUSGARTEN was established in 1999 and currently comprises seventeen sampling stations along a bathymetric and latitudinal gradient (Soltwedel et al., 2005). The focus of this study is on three sampling stations of the latitudinal transect along the 2500-m isobath: **S3**, the southernmost station, which is usually ice-free throughout the year; the central HAUSGARTEN station **HG-IV**, located close to/within the Marginal Ice Zone (MIZ) and the northernmost station **N3**, which experiences the most ice coverage (Fig. 1). The melting of sea ice in spring and summer in northern parts of the Fram Strait leads to a stratified MIZ, which is rich in nutrients and causes intense phytoplankton blooms and regionally enhanced fluxes of particulate organic matter (POM) to the seafloor (Schewe and Soltwedel, 2003; Bauerfeind et al., 2009). Annual sampling campaigns and deployments of moorings and free-falling systems at HAUSGARTEN have yielded a unique data set on faunal, bacterial, biogeochemical and geological properties as well as on hydrography and sedimentation patterns (e.g. Wlodarska-Kowalczuk et al., 2004; Hoste et al., 2007; Bauerfeind et al., 2009; Forest et al., 2010; Hasemann and Soltwedel 2011; Jacob et al., 2013; von Appen et al., 2015).

Here, we analyse sea floor images produced during three photographic surveys conducted in 2011 during the expedition ARK-XXV/2 of the German research icebreaker *Polarstern* using a towed camera system (Ocean Floor Observation System, OFOS) at HAUSGARTEN stations N3, HG-IV and S3.

2.2. OFOS specifications

The OFOS frame ($120 \times 110 \times 120$ cm) was equipped with a Canon EOS-1Ds Mark III 21 mega-pixel camera, a strobe flash (Kongsberg OE11-242), four LED lights (LED multi-Sealite, 2600 lm each), altimeter, telemetry and three red laser points (OKTOPUS), positioned 50 cm in an equilateral triangle to allow for accurate measurement of the area covered by each image. The still camera was mounted onto the steel frame so as to be positioned perpendicular to the seafloor.

The OFOS was towed for four hours at ~0.5 knots to cover a distance of 4 km at a target altitude of 1.5 m. The altitude was controlled, under instruction, by a winch operator, reacting to variations in the topography of the seafloor and sea state to maintain the target altitude. The still camera was triggered automatically at 30-s intervals to avoid spatial overlap of images and replication. Images were also manually triggered when an object/specimen of particular interest entered the field of view. These images, however, were excluded from our analysis as they introduce user bias. The details of all OFOS deployments are shown in Table 1. Physical samples obtained by Agassiz trawls and box cores enabled ground-truthing and improved the taxonomic resolution of the study (Bergmann et al., 2011).

2.3. Image selection and analysis

Each transect was divided into three equal sections nominally designated start, middle and end. This allowed us to assess potential local-scale spatial variation within each transect. Random numbers were then assigned to each of the images in a given section and the first 40 images that were appropriate for analysis (suitable lighting, no sediment clouds, not blurred) and that covered between 3.5 and 4.5 m^2 were selected.

The images were analysed in the web-2.0 based platform BIIGLE (Benthic Image Indexing and Graphical Labelling Environment) (Ontrup et al., 2009; Bergmann et al., 2011). Each image was analysed by the same taxonomic expert manually, at a zoom of 1, twice to even out learning effects. Upon completion of the second run an "area box", removing the darker, and sometimes blurred area at the edge, was placed on each image to improve the accuracy of density estimates. Only labels contained in this box were included in the final counts. The three laser points present in each image were detected by a computer algorithm (Schoening et al., 2015) and used as a standard to calculate the area of the box, which could then be used to convert taxon counts to densities. All analyses were conducted in a shaded room, to improve accuracy as external glare is reduced. The same computer/monitor set up was used in all analyses to remove variation brought about by varying resolution capabilities.

2.4. Sea–ice data and seafloor environmental data

Sea ice concentration data used in this study were obtained from the Center for Satellite Exploitation and Research (CERSAT) at the Institut Françaisde Recherche pour l'Exploitation de la Mer (IFREMER), France (Ezraty et al., 2007). Ice concentration was calculated based on the ARTIST Sea Ice (ASI) algorithm developed at the University of Bremen, Germany (Spreen et al., 2008), extracted from the X and Y position covering a 30-km^2 area above each transect. Data are available on a daily basis (01/08/2009–31/07/2011) with a 6.25×6.25 km^2 spatial resolution.

The environmental data were obtained as part of a long-term programme conducted by the German Alfred Wegener Institute Helmholtz centre for Polar and Marine Research (AWI) at HAUSGARTEN. Virtually undisturbed sediment samples were taken in 2011 using a video-guided multiple corer (TV-MUC). Cores were sub-sampled using plastic syringes (2 cm diameter) modified with

Table 1
Summary of gear deployments done at HAUSGARTEN stations. (Lat) latitude, (Lon) longitude, (OFOS) Ocean Floor Observation System, (MUC) multiple corer.

Deployment number	Sampling station	Date (dd/mm/yr)	Position Lat (N)	Position Lon (E)	Depth (m)	Gear	No. images taken (No. analysed)
PS78/0171-1	N3	27/07/2011	79° 35.84′	5° 9.95′	2788	OFOS start	
PS78/0171-1	N3	27/07/2011	79° 34.11′	5° 15.08′	2663	OFOS end	304 **(120)**
PS78/0171-6	N3	27/07/2011	79° 35.71′	5° 13.26′	2753	MUC	
PS78/0143-2	HG-IV	16/07/2011	79° 1.74′	4° 9.56′	2639	OFOS start	
PS78/0143-2	HG-IV	16/07/2011	79° 3.90′	4° 17.19′	2407	OFOS end	486 **(120)**
PS78/0143-7	HG-IV	16/07/2011	79° 3.86′	4° 10.58′	2468	MUC	
PS78/0182-1	S3	30/07/2011	78° 37.00′	5° 0.19′	2366	OFOS start	
PS78/0182-1	S3	30/07/2011	78° 36.99′	5° 9.95′	2351	OFOS end	365 **(120)**
PS78/0182-3	S3	30/07/2011	78° 36.38′	5° 3.92′	2341	MUC	

the anterior ends cut off and sub-divided into 1-cm layers. Chlorophyll *a* and its degradation products (phaeopigments) were analysed using a Turner fluorometer (Thiel, 1978). The bulk of pigments (chloroplastic pigment equivalents, CPE) indicate food availability from photosynthetically derived material reaching the seafloor. Phospholipids, representative for the total microbial biomass, were analysed photometrically. Proteins (readily soluble per sediment volume) were also analysed photometrically and are indicative of living and dead biomass (organisms and detrital matter within the sediments). Porosity was assessed by the weight loss of wet sediment samples when dried at 60 °C. For this study, the measurements in the top five 1-cm layers (Jacob et al., 2013; Górska et al., 2014) were used to create boxplots of the environmental characteristics at each station. Locations of all MUC deployments can be found in Table 1.

Environmental variables (i.e. biogenic habitat features) that were recorded alongside the megafaunal abundances for each image included: *Caulophacus* debris, *Bathycrinus* stalks, *Pourtalesia jeffreysi* tests, burrows, Lebensspuren, dropstones (large stones), pebbles (small stones), anthropogenic litter, shells and bone material.

2.5. Data analysis

The megafaunal abundances for each image were extracted from BIIGLE and converted to density (abundance ind. m^{-2}) using. Standard (non-) parametric tests (Minitab 17: one-way analysis of variance with Tukey comparisons, Kruskal-Wallis test) were used to compare the densities and environmental parameters between the stations. If non-parametric tests had to be used, due to non-homogenous variance, pairwise Mann-Whitney *U*-tests were applied using a Bonferroni correction (p=0.05/3 (comparisons)= 0.0167).

Biota were also grouped in terms of feeding type i.e. predator/scavenger, deposit feeder, suspension feeder and 'not defined' (n.d) based on information in the literature and advice from specialists (Bergmann et al., 2009).

Shannon-Wiener diversity and Pielou's evenness was computed for each image to compare the indices from different sections and stations. Since Whittaker (1960) first defined species diversity in terms of α (the mean diversity observed within an individual habitat), β (the diversity differential amongst habitats, i.e. species turnover) and γ diversities (the overall diversity observed in the ecosystem as a whole) there has been much debate on exactly how these diversities should be calculated, particularly between multiplicative and additive diversity partitioning, with Veech and Crist (2010) showing both methods to be statistically valid and logically sound. In this study, we use an additive diversity partition (Crist and Veech, 2006; Zhang et al., 2014), since this allows direct comparison between α and β diversity as they are expressed in the same unit. We describe α, β and γ diversity as:

- α diversity as the mean species number (S) m^{-2} at each station/section i.e. $\alpha = \frac{1}{n}\sum_{\text{image1}}^{\text{imagen}} \frac{S}{\text{image area}}$
- γ diversity as the total species richness ($S_{\max}$) at each station/site m^{-2} i.e. $\gamma = \frac{1}{n}\sum_{\text{image1}}^{\text{imagen}} \frac{S_{\max}}{\text{image area}}$
- β diversity as the species turnover at a site, therefore the difference between the total species richness and the observed species richness i.e. $\beta = \gamma - \alpha$

Routines from multivariate statistics (PRIMER-e 6.1.6, Clarke and Gorley (2006)) were used to determine differences in the taxonomic composition based on Bray-Curtis similarity analysis. All density data were square-root transformed to counteract the effect of very abundant taxa. The similarities of different images and transects were depicted in an ordination biplot (MDS, non-metric multi-dimensional scaling), with each point relating to a single photograph. A two-way nested ANOSIM routine was used to assess differences in species composition between stations and sections of transects, whereas a one-way ANOSIM routine was used to test for differences within each transect. The SIMPER module was used to identify the discriminator species between sections and stations. To determine the key biogenic habitat features that accounted for species composition and to what extent these variables affected species composition the BIOENV module was applied.

3. Results

In total, 352 images were analysed. **N3**: Start=40, Middle=40, End=40; **HG-IV**: Start=40, Middle=40, End=40; **S3**: Start=32, Middle=40, End=40. The area analysed comprised 1260.4 m^2 in total (**N3**=430.6 m^2, **HG-IV**=449.6 m^2, **S3**=380.2 m^2) with mean areas of **N3**=3.81 ± 0.035 m^2 (SEM), **HG-IV**=3.78 ± 0.036 m^2 and **S3**=3.59 ± 0.043 m^2.

3.1. Taxa recorded

A total of 29 taxa and morphotypes were recorded in the images and of these, 18 were identified to species level. In addition, ten biogenic habitat features were labelled. For all statistical analysis, only those 21 larger taxa or morphotypes that could be identified with the highest degree of certainty were included (Fig. 2), while all taxa/morphotypes were included in calculations of the total megafaunal abundance. The species accumulation curves (Fig. 3) show that the selected sample size in each section is suitable as the line heads towards a plateau before the 40-image mark. Taxonomic resolution was increased compared with previous work (Bergmann et al., 2011) as further ground-truthing by trawls and box cores enabled the identification of: *Neohela lamia* (previously: burrowing crustacean), *Byglides groenlandicus* (flattish worm), *Halirages cainae* (amphipod) and *Poliometra prolixa* (comatulid). The hydroid *Candelabrum* spp.is a new addition to the HAUSGARTEN taxonomic inventory and only occurred at the northernmost station. *Cladorhiza gelida* appears to be the most common cladorhizid at HAUSGARTEN, although a less common congener, *C. abyssicola*, was also recently identified from this region (Pantke, 2014).

3.2. Regional-scale variation

3.2.1. Species composition and abundances

There were significant differences in total megafaunal abundance at different stations (χ^2=250.08, df=2), with mean values of 26.74 ± 0.63 (SEM) at N3, 11.21 ± 0.25 at HG-IV and 18.34 ± 0.39 individuals m^{-2} at S3 (Fig. 4). When broken down into categories describing broad feeding type, we found significant differences in the densities of predator/scavengers between N3 and HG-IV/S3 (χ^2=213.37, df=2) and between all stations for suspension feeders (χ^2=117.90, df=2) and deposit feeders (χ^2=250.49, df=2) (Table 2).

A two-way ANOSIM with sections nested within stations produced a Global R of 0.298 (p=0.001) for sections and 0.704 (p=0.021) for stations. This shows that every section of each transect was significantly similar in species composition whereas the different stations as a whole were significantly different. In the pairwise tests between stations the largest difference was found between N3 and S3 (R=1, p=0.001) followed by N3 and HG-IV (R=0.630, R=0.001) and S3 and HG-IV (R=0.407, p=0.001) (Table 3). An MDS plot (Fig. 5) also documents a distinct separation between the species composition at each station.

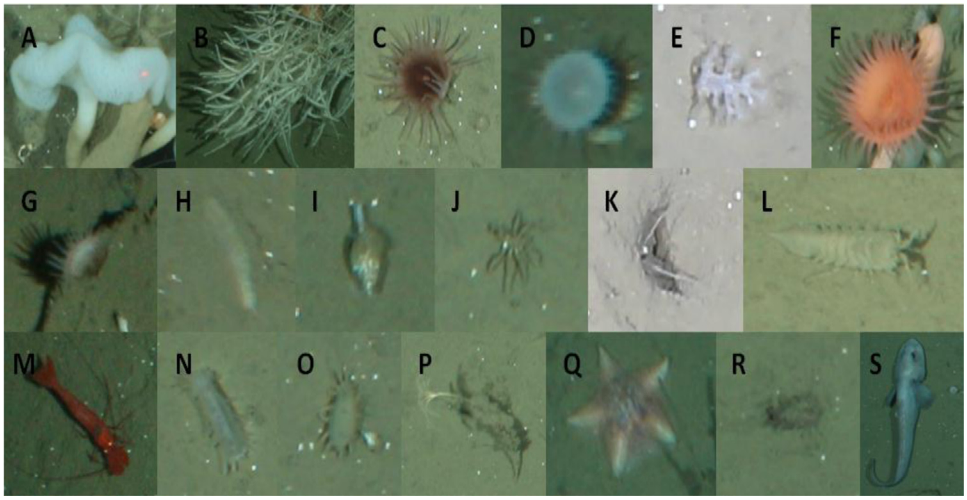

Fig. 2. Examples of taxa/morphotypes from HAUSGARTEN stations N3, HG-IV and S3 used in statistical analysis tests: (A) *Caulophacus arcticus*, (B) *Cladorhiza* cf. *gelida*, (C) purple actinarian, (D) cf. *Bathyphellia margaritacea*, (E) *Gersemia fruticosa*, (F) *Hormathiidae*, (G) white long-tentacled actinarian, (H) *Byglides groenlandicus*, (I) *Mohnia* spp., (J) *Ascorhynchus abyssi*, (K) *Neohela lamia*, (L) *Saduria megalura*, (M) *Bythocaris* spp., (N) *Kolga hyalina*, (O) *Elpidia heckeri*, (P) *Bathycrinus carpenterii*, (Q) *Hymenaster pellucidus*, (R) *Pourtalesia jeffreysi*, (S) *Lycodes frigidus*.

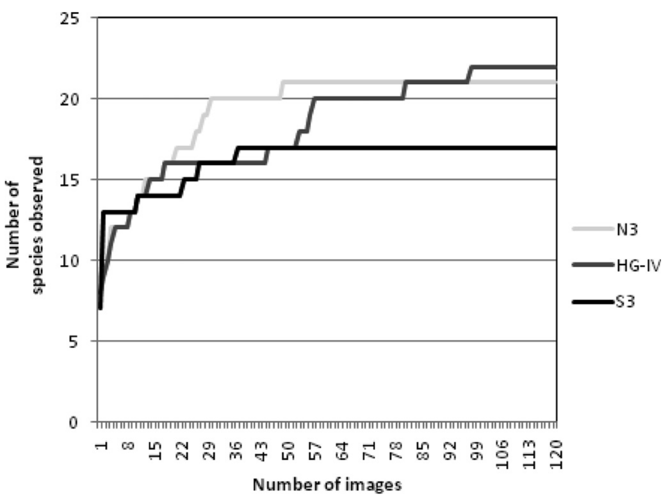

Fig. 3. Species accumulation curves for the 120 images from photographic transects taken at HAUSGARTEN stations N3, HG-IV and S3.

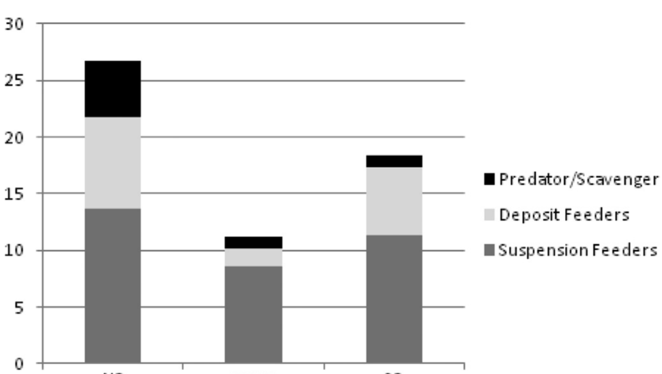

Fig. 4. Mean densities of organisms (ind. m^{-2}) belonging to different feeding types recorded from photographic transects taken at HAUSGARTEN stations N3, HG-IV and S3.

The SIMPER routine revealed the dominant species contributing to the dissimilarity between the stations. Images of N3 had the highest mean similarity (80.1%) of the three stations, followed by S3 (64.4%) and HG-IV (56.1%). The main species contributing to the difference seen between the communities at N3 and HG-IV/S3 is the sea cucumber *Kolga hyalina*. Its mean abundance was 40 times higher at N3 than at HG-IV, whereas they were completely absent at S3. Kruskal-Wallis/Mann-Whitney U-tests show this difference in abundances to be significant between all three sites ($\chi^2=287.93$, df=2). The next dominant organisms to cause the greatest dissimilarity between N3 and HG-IV/S3 was the whelk *Mohnia* spp. and the sea lily *Bathycrinus carpenterii*. Moreover, there was a significant difference in the abundance of *Mohnia* spp. between N3 and HG-IV/S3 ($\chi^2=219.46$, df=2) and *B. carpenterii* between all stations ($\chi^2=197.66$, df=2). *Mohnia* spp. densities were highest at N3 followed by HG-IV and S3. *B. carpenterii* densities displayed the opposite trend with the greatest quantity being observed at S3 followed by HG-IV and N3 (Table 2). The top three species accounting for dissimilarity between HG-IV and S3 were the soft coral *Gersemia fruticosa, B. carpenterii* and the smaller-sized sea cucumber *Elpidia heckeri. Gersemia fruticosa* ($\chi^2=187.15$, df=2) and *E. heckeri* ($\chi^2=101.01$, df=2) also showed significant differences in abundance at each station with higher desities observed at S3 (Table 2).

In terms of diversity measures, the megafauna of N3 was characterised by a significantly higher Shannon-Wiener index compared to HG-IV and S3 ($\chi^2=49.73$, df=2) and Pielou's evenness was also significantly higher at N3, followed by significantly lower evenness at HG-IV and S3 ($\chi^2=112.78$, df=2). Significant differences were seen in the α and β diversities between each station with S3 also showing a significantly greater γ diversity when compared with N3 and HG-IV (Table 2). The α/β diversity contributions to overall γ diversity were 79.89/20.11% at N3, 62.27/37.73% at HG-IV and 73.59/26.41% at S3.

An MDS plot of the biogenic habitat features labelled did not show large variations as to the physical environment at each station (Fig. 6). This is supported through the pairwise comparisons of the ANOSIM test (Table 3) with the largest value coming in the comparison between N3 and HG-IV ($R=0.284$, $p=0.001$). However, whilst there was no significant difference in the overall composition of the physical environment between each station, there were several significant differences in the abundances of which feature occurred at each station. Station N3 harboured significantly fewer burrows ($\chi^2=145.58$, df=2) than HG-IV/S3 as well as significantly higher quantities of pebbles ($\chi^2=113.82$, df=2), indicating a greater proportion of hard substrata. When it comes to the environmental characteristics that are most important in describing species composition, burrows showed the strongest correlation with a BIOENV value of 0.318.

Table 2
Mean densities (ind. m^{-2}) of megafaunal taxa/morphotypes, biogenic habitat features, and diversity indices recorded from photographic transects at HAUSGARTEN stations N3, HG-IV and S3.

Taxon	FT	N3 mean	± SE	HG-IV mean	± SE	S3 mean	± SE	Test used	p	f or χ^2	Significant difference
Porifera											
_Caulophacus arcticus_*	SF	0.520	0.094	0.064	0.015	0.018	0.007	K-W, M-W	< 0.0005	62.50	N3 v HG-IV, N3 v S3, HG-IV v S3
Cladorhiza cf. _gelida_*	SF	0.123	0.019	0.070	0.014	0.076	0.016	K-W, M-W	0.030	6.99	No (Bonferroni)
Small round sponge	SF	6.825	0.271	3.136	0.181	6.351	0.176	K-W, M-W	< 0.0005	128.88	N3 v HG-IV, HG-IV v S3
Sponge morphotype 2	SF	0.229	0.057	0.101	0.035			K-W, M-W	< 0.0005	24.49	N3 v HG-IV, N3 v S3, HG-IV v S3
Cnidaria											
Purple actinarian*	SF	0.007	0.004	0.368	0.039	0.241	0.028	K-W, M-W	< 0.0005	90.06	N3 v HG-IV, N3 v S3
cf. _Bathyphellia margaritacea_*	SF	1.643	0.076	2.457	0.121	1.998	0.092	K-W, M-W	< 0.0005	24.60	N3 v HG-IV, N3 v S3, HG-IV v S3
_Gersemia fruticosa_*	SF	0.002	0.002	0.190	0.043	0.751	0.055	K-W, M-W	< 0.0005	187.15	N3 v HG-IV, N3 v S3, HG-IV v S3
Candelabrum spp.*	P/S	0.003	0.003					K-W, M-W	0.408	1.76	No
Hormathiidae*	SF	0.100	0.018	0.265	0.043	0.441	0.075	K-W, M-W	< 0.0005	21.60	N3 v HG-IV, N3 v S3
White long-tentacled actinarian*	SF	0.113	0.018	0.119	0.021	0.465	0.050	K-W, M-W	< 0.0005	54.63	N3 v S3, HG-IV v S3
Ceriantharia	SF					0.029	0.017	ANOVA	0.071	2.67	No
Actinaria	SF			0.019	0.007	0.003	0.003	K-W, M-W	0.007	10.01	N3 v HG-IV, N3 v S3
Annelida											
_Byglides groenlandicus_*	P/S	0.029	0.009	0.071	0.014	0.085	0.018	K-W, M-W	0.015	8.36	N3 v HG-IV, N3 v S3
Mollusca											
Mohnia spp.*	P/S	3.884	0.154	0.707	0.051	0.555	0.040	K-W, M-W	< 0.0005	219.46	N3 v HG-IV, N3 v S3
Pycnogonida											
_Ascorhynchus abyssi_*	P/S	1.008	0.073	0.242	0.028	0.329	0.035	K-W, M-W	< 0.0005	104.36	N3 v HG-IV, N3 v S3, HG-IV v S3
Crustacea											
_Neohela lamia_*	DF	0.009	0.006	0.338	0.051	0.268	0.032	K-W, M-W	< 0.0005	72.46	N3 v HG-IV, N3 v S3
_Saduria megalura_*	n.d.	0.010	0.005	0.005	0.003	0.017	0.006	K-W, M-W	0.166	3.56	No
Bythocaris spp.*	P/S	0.049	0.011	0.068	0.016	0.027	0.010	K-W, M-W	0.073	11.92	HG-IV v S3
Verum striolatum	SF	0.004	0.004	0.005	0.003			K-W, M-W	0.410	1.78	No
Isopoda	DF	2.435	0.125	0.614	0.040	4.731	0.159	K-W, M-W	< 0.0005	242.40	N3 v HG-IV, N3 v S3, HG-IV v S3
Birsteiniamysis inermis	n.d.			0.034	0.009	0.058	0.012	ANOVA	< 0.0005	10.45	N3 v HG-IV, N3 v S3
Halirages cainae	n.d.			0.002	0.002	0.021	0.007	ANOVA	< 0.0005	8.76	N3 v S3, HG-IV v S3
Echinodermata											
_Kolga hyalina_*	DF	4.493	0.123	0.098	0.020			K-W, M-W	< 0.0005	287.93	N3 v HG-IV, N3 v S3, HG-IV v S3
_Elpidia heckeri_*	DF	1.117	0.053	0.387	0.040	0.828	0.055	K-W, M-W	< 0.0005	101.01	N3 v HG-IV, N3 v S3, HG-IV v S3
_Bathycrinus carpenterii_*	SF	4.074	0.122	1.772	0.121	0.836	0.049	K-W, M-W	< 0.0005	197.66	N3 v HG-IV, N3 v S3, HG-IV v S3
_Hymenaster pellucidus_*	P/S	0.013	0.005	0.007	0.004	0.207	0.023	K-W, M-W	0.165	3.60	No
_Pourtalesia jeffreysi_*	DF	0.048	0.012	0.050	0.013	0.207	0.023	K-W, M-W	< 0.0005	60.23	N3 v S3, HG-IV v S3
_Poliometra prolixa_*	SF			0.009	0.005			ANOVA	0.024	3.69	No (Bonferroni)
Pisces											
_Lycodes frigidus_*	P/S			0.004	0.003	0.005	0.003	ANOVA	0.360	1.02	No
Feeding type											
Predator/scavengers		4.985	0.199	1.104	0.071	1.003	0.056	K-W, M-W	< 0.0005	213.37	N3 v HG-IV, N3 v S3
Suspension feeders		13.642	0.387	8.574	0.202	11.208	0.270	K-W, M-W	< 0.0005	117.9	N3 v HG-IV, N3 v S3, HG-IV v S3
Deposit feeders		8.102	0.183	1.486	0.083	6.034	0.170	K-W, M-W	< 0.0005	250.49	N3 v HG-IV, N3 v S3, HG-IV v S3
Not defined		0.010	0.005	0.041	0.010	0.096	0.017	K-W, M-W	< 0.0005	26.81	N3 v HG-IV, N3 v S3, HG-IV v S3
Overall densities		26.740	0.630	11.206	0.246	18.341	0.389	K-W, M-W	< 0.0005	250.08	N3 v HG-IV, N3 v S3, HG-IV v S3
Diversity indices											
Shannon-Wiener H		1.952	0.011	1.771	0.025	1.820	0.018	K-W, M-W	< 0.0005	49.73	N3 v HG-IV, N3 v S3
Pilou's evenness J		0.848	0.003	0.802	0.006	0.763	0.005	K-W, M-W	< 0.0005	112.78	N3 v HG-IV, N3 v S3, HG-IV v S3
α Diversity		2.694	0.050	2.502	0.068	3.124	0.066	K-W, M-W	< 0.0005	50.79	N3 v HG-IV, N3 v S3, HG-IV v S3
γ Diversity		3.710	0.035	4.018	0.043	4.245	0.050	K-W, M-W	< 0.0005	58.65	N3 v S3, HG-IV v S3
β Diversity		1.016	0.037	1.516	0.051	1.121	0.051	K-W, M-W	< 0.0005	59.19	N3 v HG-IV, N3 v S3, HG-IV v S3
Environmental variables											
Caulophacus debris		0.834	0.088	0.162	0.026	0.151	0.024	K-W, M-W	< 0.0005	78.32	N3 v HG-IV, N3 v S3
Bathycrinus stalks		1.798	0.085	1.420	0.093	0.439	0.041	K-W, M-W	< 0.0005	125.73	N3 v HG-IV, N3 v S3, HG-IV v S3
Pourtalesia test		0.195	0.030	0.160	0.038	0.158	0.028	K-W, M-W	0.366	2.01	No
Burrows		0.149	0.028	3.739	0.436	1.673	0.101	K-W, M-W	< 0.0005	145.58	N3 v HG-IV, N3 v S3
Lebensspuren		15.395	0.206	14.581	0.176	16.072	0.302	K-W, M-W	< 0.0005	19.52	N3 v HG-IV, HG-IV v S3

Table 2 (*continued*)

Taxon	FT	N3 mean	± SE	HG-IV mean	± SE	S3 mean	± SE	Test used	*p*	*f* or χ^2	Significant difference
(Drop) stone		0.110	0.019	0.098	0.017	0.118	0.021	ANOVA	0.710	0.34	No
Anthropogenic litter		0.002	0.002	0.014	0.005			K-W, M-W	0.017	8.16	No (Bonferroni)
Shell		0.851	0.057	0.172	0.023	0.063	0.014	K-W, M-W	<0.0005	158.65	N3 v HG-IV, N3 v S3, HG-IV v S3
Pebble		17.106	1.624	3.831	0.549	1.049	0.103	K-W, M-W	<0.0005	113.82	N3 v HG-IV, N3 v S3
Bone		0.187	0.025	0.024	0.008			K-W, M-W	<0.0005	84.72	N3 v HG-IV, N3 v S3, HG-IV v S3

(FT) feeding type (P/S; predator/scavenger, DF; deposit feeder, SF; suspension feeder and n.d.; not defined)
(SE) standard error; *f* or χ^2; test statistics of ANOVA or Kruskal-Wallis tests.
* indicates taxa/morphotype used for statistical analysis tests.

Table 3
ANOSIM results of community and biogenic habitat feature composition of HAUSGARTEN stations N3, HG-IV and S3.

Stations compared	ANOSIM community composition	ANOSIM biogenic habitat feature composition
N3 v HG-IV	1.000	0.284
N3 v S3	0.630	0.182
HG-IV v S3	0.407	0.106

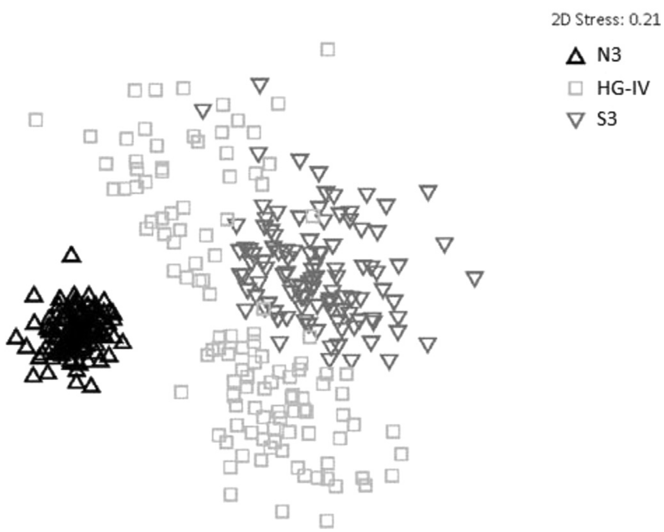

Fig. 5. MDS plot depicting community composition from photographic transects taken at HAUSGARTEN stations N3, HG-IV and S3 (each point relates to one image).

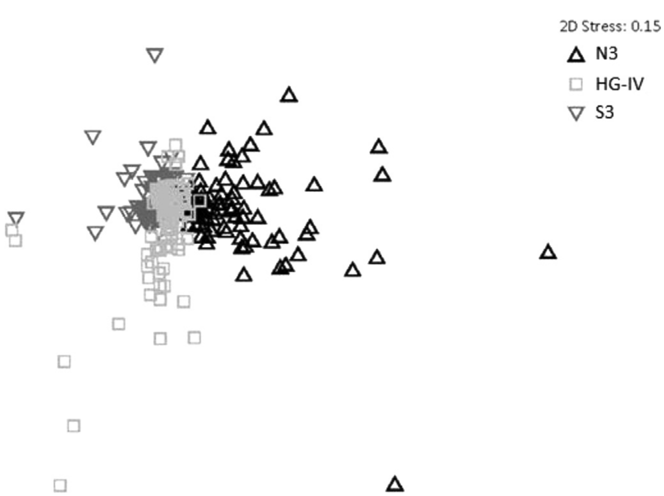

Fig. 6. MDS plot depicting benthic habitat feature composition from photographic transects taken at HAUSGARTEN stations N3, HG-IV and S3.

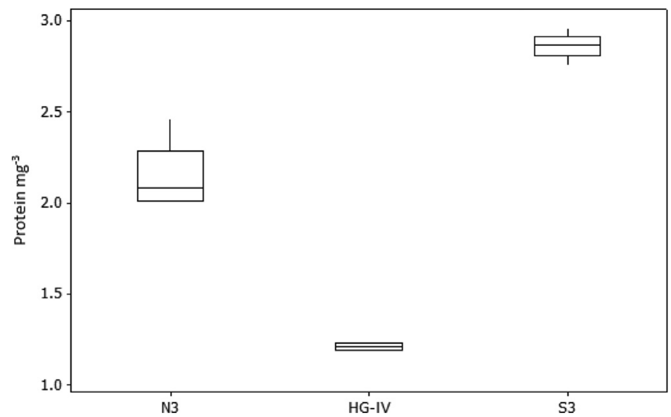

Fig. 7. Boxplot, showing the interquartile range and median protein concentrations in sediments from HAUSGARTEN stations N3, HG-IV and S3. Sediment protein concentrations indicate the biomass of small organisms and detrital matter.

Table 4
ANOSIM results of community composition within transects taken from photographic transects at HAUSGARTEN stations N3, HG-IV and S3.

Sections compared	N3	HG-IV	S3
Start v Middle	0.353	0.574	0.102
Start v End	0.376	0.884	0.136
Middle v End	0.031	0.288	0.047

3.2.2. Sea–ice and environmental data

Between August 2009 and July 2011, there were a total of 41, 22 and 2 days of ice concentration greater than 20%, in a 30-km^2 area above N3, HG-IV and S3, respectively, showing a significantly lower ice coverage towards the south (K-W, M-W, $p=<0.0005$, $\chi^2=106.50$, df=2).

Of the six sediment parameters measured in 2011 (chlorophyll *a*, chloroplastic pigment equivalent (CPE), phaeopigments, proteins, phospholipids, porosity) only protein concentrations were significantly different (ANOVA, $p<0.0005$, $F=251.73$, df=2) (Fig. 7).

3.3. Local-scale variations

3.3.1. HG-IV

There were significant differences between the community compositions of the start, middle and end of the HG-IV transect. A global *R* value of 0.574 ($p=0.001$) (Table 4) indicates dissimilarity in the community composition of the start and middle of the transect which is primarily caused by *Bathycrinus carpenterii*, cf. *Bathyphellia margaritacea* and a purple actinarian showing greater densities in the middle section and *Mohnia* spp. and *K. hyalina* showing greater densities in the start section (SIMPER). An *R* (ANOSIM) of 0.884 ($p=0.001$) for the start and end indicates two almost separate communities, which is primarily caused by *B.*

Table 5
Mean densities (ind m^{-2}) of megafaunal taxa/morphotypes, biogenic habitat features and diversity indices recorded from different sections of the photographic transect taken at HAUSGARTEN station HG-IV.

Taxon	FT	Start mean	± SE	Middle mean	± SE	End mean	± SE	Test used	p	f or χ^2	Significant difference
Porifera											
Caulophacus arcticus*	SF			0.058	0.024	0.131	0.034	ANOVA	0.001	7.34	Start v End
Cladorhiza cf. gelida	SF	0.027	0.017	0.071	0.023	0.109	0.031	K-W, M-W	0.055	5.82	No
Small round sponge	SF	4.945	0.229	3.253	0.239	1.254	0.123	K-W, M-W	< 0.0005	76.42	Start v Middle, Start v End, Middle v End
Sponge morphotype 2	SF			0.057	0.043	0.245	0.091	ANOVA	0.010	4.80	Start v End
Cnidaria											
Purple actinarian*	SF	0.044	0.022	0.405	0.059	0.646	0.073	K-W, M-W	< 0.0005	50.38	Start v Middle, Start v End, Middle v End
cf. Bathyphellia margaritacea*	SF	2.018	0.153	3.047	0.228	2.295	0.210	ANOVA	0.001	7.07	Start v Middle
Gersemia fruticosa*	SF	0.013	0.009	0.025	0.012	0.527	0.109	K-W, M-W	< 0.0005	43.34	Start v End, Middle v End
Hormathiidae*	SF	0.276	0.054	0.166	0.052	0.354	0.105	K-W, M-W	0.083	4.97	No
White long-tentacled actinarian*	SF	0.166	0.033	0.137	0.049	0.056	0.023	K-W, M-W	0.018	8.03	No (Bonferroni)
Actinaria	SF					0.055	0.019	ANOVA	0.001	7.99	Start v End, Middle v End
Annelida											
Byglides groenlandicus*	P/S	0.138	0.030	0.062	0.024	0.013	0.009	K-W, M-W	< 0.0005	15.97	Start v Middle, Start v End
Mollusca											
Mohnia spp.*	P/S	0.996	0.077	0.739	0.098	0.392	0.055	K-W, M-W	< 0.0005	29.96	Start v Middle, Start v End, Middle v End
Pycnogonida											
Ascorhynchus abyssi*	P/S	0.447	0.054	0.255	0.041	0.027	0.013	K-W, M-W	< 0.0005	41.48	Start v Middle, Start v End, Middle v End
Crustacea											
Neohela lamia*	DF			0.186	0.048	0.820	0.110	K-W, M-W	< 0.0005	73.39	Start v End, Middle v End
Saduria megalura*	n.d.	0.007	0.007	0.007	0.007			ANOVA	0.604	0.51	No
Bythocaris spp.*	P/S	0.020	0.012	0.045	0.019	0.138	0.042	K-W, M-W	0.009	9.42	Start v End
Verum striolatum	SF	0.007	0.007	0.007	0.007			ANOVA	0.604	0.51	No
Isopoda	DF	0.738	0.082	0.615	0.068	0.491	0.048	K-W, M-W	0.134	4.02	No
Birsteiniamysis inermis	n.d.	0.020	0.011	0.025	0.015	0.058	0.019	K-W, M-W	0.122	4.21	No
Halirages cainae	n.d.					0.007	0.007	ANOVA	0.376	0.99	No
Echinodermata											
Kolga hyalina*	DF	0.298	0.046					ANOVA	< 0.0005	42.68	Start v Middle, Start v End
Elpidia heckeri*	DF	0.280	0.047	0.303	0.042	0.576	0.095	K-W, M-W	0.090	4.82	No
Bathycrinus carpenterii*	SF	0.304	0.050	2.140	0.108	2.835	0.180	K-W, M-W	< 0.0005	80.32	Start v Middle, Start v End, Middle v End
Hymenaster pellucidus*	P/S			0.007	0.007	0.014	0.010	ANOVA	0.379	0.98	No
Pourtalesia jeffreysi *	DF	0.077	0.032	0.037	0.037	0.037	0.019	K-W, M-W	0.409	1.79	No
Poliometra prolixa*	SF	0.006	0.006			0.022	0.012	ANOVA	0.135	2.04	No
Pisces											
Lycodes frigidus*	P/S			0.006	0.006	0.006	0.006	ANOVA	0.615	0.49	No
Feeding types											
Predator/scavengers		1.602	0.112	1.115	0.121	0.608	0.081	ANOVA	< 0.0005	21.92	Start v Middle, Start v End, Middle v End
Suspension feeders		7.806	0.308	9.367	0.314	8.530	0.386	ANOVA	0.006	5.30	Start v Middle
Deposit feeders		1.393	0.115	1.140	0.084	1.925	0.187	K-W, M-W	0.009	9.41	Middle v End
Not defined		0.027	0.013	0.031	0.016	0.065	0.012	ANOVA	0.198	1.64	No
Overall densities		10.828	0.410	11.653	0.316	11.127	0.527	K-W, M-W	0.184	3.38	No
Diversity indices											
Shannon-Wiener H		1.629	0.035	1.737	0.037	1.943	0.043	ANOVA	< 0.0005	17.10	Start v End, Middle v End
Pilou's evenness J		0.758	0.010	0.805	0.008	0.841	0.010	ANOVA	< 0.0005	20.66	Start v Middle, Start v End
α Diversity		2.272	0.085	2.285	0.088	2.944	0.138	K-W, M-W	< 0.0005	17.53	Start v End, Middle v End
γ Diversity		3.111	0.037	3.617	0.041	4.286	0.099	K-W, M-W	0.001	13.16	Start v End, Middle v End
β Diversity		0.839	0.067	1.332	0.087	1.342	0.100	ANOVA	0.049	3.10	No (Bonferroni)

Table 5 (*continued*)

Taxon	FT	Start mean	±SE	Middle mean	±SE	End mean	±SE	Test used	p	f or χ^2	Significant difference
Environmental variables											
Caulophacus debris		0.012	0.008	0.172	0.041	0.291	0.057	K-W, M-W	< 0.0005	23.22	Start v Middle, Start v End
Bathycrinus stalks		0.438	0.068	1.534	0.100	2.193	0.154	K-W, M-W	< 0.0005	69.11	Start v Middle, Start v End, Middle v End
Pourtalesia tests		0.196	0.103	0.222	0.043	0.054	0.017	K-W, M-W	0.004	10.91	Start v Middle, Middle v End
Burrows		0.285	0.047	1.316	0.207	9.343	0.610	K-W, M-W	< 0.0005	80.00	Start v Middle, Start v End, Middle v End
Lebensspuren		13.967	0.432	13.930	0.168	15.103	0.557	K-W, M-W	0.044	6.26	No (Bonferroni)
(Drop) stone		0.018	0.010	0.082	0.023	0.188	0.039	K-W, M-W	< 0.0005	16.67	Start v Middle, Start v End
Anthropogenic litter		0.019	0.011			0.021	0.012	ANOVA	0.206	1.60	No
Shells		0.114	0.031	0.238	0.045	0.153	0.039	ANOVA	0.076	2.63	No
Pebbles		0.228	0.044	0.380	0.056	10.604	0.909	K-W, M-W	< 0.0005	73.08	Start v End, Middle v End
Bone		0.014	0.010	0.026	0.013	0.023	0.018	K-W, M-W	0.729	0.63	No

(FT) feeding type (P/S; predator/scavenger, DF; deposit feeder, SF; suspension feeder, n.d.; not defined)
(SE) standard error; *f* or χ^2; test statistics of ANOVA or Kruskal-Wallis tests.
* indicates taxa/morphotype used for statistical analysis tests.

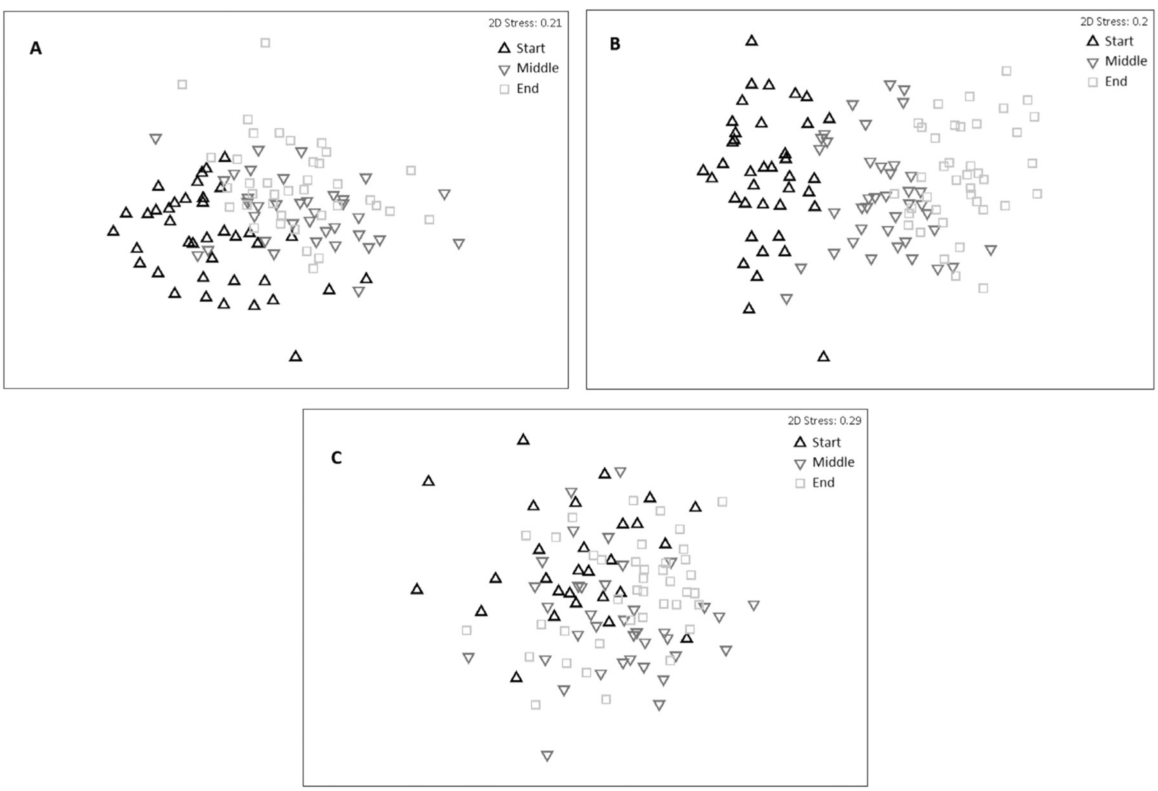

Fig. 8. MDS plot depicting within transect (sections: Start, Middle and End) community composition from photographic transects taken at HAUSGARTEN stations (A) N3, (B) HG-IV and (C) S3.

carpenterii, the burrowing amphipod *Neohela lamia* and a purple actinarian with greater densities in the end section and the pycnogonid *Ascorhynchus abyssi* and *Mohnia* spp. with greater densities in the end section (SIMPER). The species composition of the transect middle and end were hardly different (ANOSIM; $R=0.288$, $p=0.001$).

The overall megafaunal abundance of the three transect sections did not differ significantly (Table 5). However, there was a significant decrease in the number of predator/scavengers ($F=21.92$, df=2) along the transect, with an increase in suspension feeders ($F=5.30$, df=2) between the start and middle sections and an increase in deposit feeders ($\chi^2=9.41$, df=2) between the middle and end sections.

The Shannon-Wiener index shows a significant increase in the end section compared to the start and middle ($F=17.10$, df=2), and Pielou's evenness was significantly lower in the start section compared with the middle and end ($F=20.66$, df=2). Although the start section also shows a significant difference in α ($\chi^2=17.53$, df=2) and γ ($\chi^2=13.16$, df=2) diversity, no significant difference in β diversity was observed. The overall α/β diversity contributions to overall γ diversity were 73.03/26.97%, 63.17/36.83% and 68.68/31.32% in the start, middle and end sections, respectively. The comparison of the ten biogenic habitat features indicate low dissimilarity (ANOSIM; Global $R=0.302$, $p=0.001$).

3.3.2. N3 and S3

There was no significant difference in community composition at N3 (one way ANOSIM, Global $R=0.254$, $p=0.001$). This result is illustrated by the MDS plot (Fig. 8), with moderate overlap

Table 6
Mean densities (ind. m^{-2}) of megafaunal taxa/morphotypes, biogenic habitat features and diversity indices recorded from different sections of the photographic transect taken at HAUSGARTEN station N3.

Taxon	FT	Start mean	±SE	Middle mean	±SE	End mean	±SE	Test used	*p*	*f* or χ^2	Significant difference
Porifera											
*Caulophacus arcticus**	SF	0.348	0.189	0.887	0.182	0.350	0.084	K-W, M-W	< 0.0005	15.82	Start v Middle, Middle v End
Cladorhiza cf. *gelida* *	SF	0.098	0.026	0.086	0.027	0.182	0.040	K-W, M-W	0.109	4.44	No
Small round sponge	SF	4.397	0.219	7.914	0.428	8.286	0.439	K-W, M-W	< 0.0005	57.89	Start v Middle, Start v End
Sponge morphotype 2	SF	0.085	0.036	0.103	0.054	0.497	0.148	K-W, M-W	0.004	11.01	Start v End, Middle v End
Cnidaria											
Purple actinarian*	SF	0.013	0.009	0.008	0.008			ANOVA	0.401	0.92	No
cf. *Bathyphellia margaritacea**	SF	1.769	0.146	1.627	0.119	1.529	0.128	ANOVA	0.428	0.86	No
*Gersemia fruticosa**	SF	0.007	0.007					ANOVA	0.391	0.95	No
Candelabrum spp.*	P/S			0.008	0.008			ANOVA	0.346	1.07	No
Hormathiidae*	SF	0.013	0.009	0.127	0.037	0.164	0.034	K-W, M-W	< 0.0005	18.08	Start v Middle, Start v End
White long-tentacled actinarian*	SF	0.136	0.030	0.129	0.038	0.074	0.025	ANOVA	0.307	1.19	No
Annelida											
*Byglides groenlandicus**	P/S	0.032	0.013	0.026	0.019	0.029	0.014	ANOVA	0.969	0.03	No
Mollusca											
Mohnia spp.*	P/S	2.866	0.170	4.461	0.291	4.381	0.254	K-W, M-W	< 0.0005	30.41	Start v Middle, Start v End
Pycnogonida											
*Ascorhynchus abyssi**	P/S	0.570	0.082	1.097	0.096	1.374	0.155	K-W, M-W	< 0.0005	26.82	Start v Middle, Start v End
Crustacea											
*Neohela lamia**	DF	0.006	0.006	0.009	0.009	0.013	0.013	K-W, M-W	0.998	0.00	No
*Saduria megalura**	n.d.	0.007	0.007			0.024	0.013	K-W, M-W	0.171	3.54	No
Bythocaris spp.*	P/S	0.038	0.015	0.043	0.019	0.065	0.022	ANOVA	0.566	0.57	No
Verum striolatum	SF			0.013	0.013			ANOVA	0.346	1.07	No
Isopoda	DF	1.420	0.122	3.049	0.226	2.895	0.189	K-W, M-W	< 0.0005	41.80	Start v Middle, Start v End
Echinodermata											
*Kolga hyalina**	DF	5.090	0.197	4.361	0.184	4.005	0.221	ANOVA	0.001	7.69	Start v End
*Elpidia heckeri**	DF	0.932	0.075	1.366	0.086	1.071	0.098	ANOVA	0.002	6.43	Start v Middle
*Bathycrinus carpenterii**	SF	4.128	0.193	4.149	0.270	3.949	0.172	K-W, M-W	0.913	0.18	No
*Hymenaster pellucidus**	P/S	0.031	0.013			0.007	0.007	ANOVA	0.036	3.42	No (Bonferroni)
*Pourtalesia jeffreysi**	DF	0.019	0.014	0.090	0.028	0.038	0.020	K-W, M-W	0.035	6.69	No (Bonferroni)
Feeding types											
Predator/scavengers		3.537	0.203	5.636	0.325	5.856	0.357	K-W, M-W	< 0.0005	34.95	Start v Middle, Start v End
Suspension feeders		10.993	0.430	15.044	0.613	15.032	0.720	K-W, M-W	< 0.0005	33.79	Start v Middle, Start v End
Deposit feeders		7.467	0.232	8.875	0.317	8.021	0.357	ANOVA	0.006	5.35	Start v Middle
Not defined		0.007	0.007			0.023	0.013	ANOVA	0.153	1.91	No
Overall densities		22.004	0.587	29.556	1.046	28.932	1.131	K-W, M-W	< 0.0005	250.08	Start v Middle, Start v End
Diversity indices											
Shannon-Wiener ***H***		1.912	0.016	1.984	0.019	1.964	0.022	ANOVA	0.023	3.90	No (Bonferroni)
Pilou's evenness ***J***		0.848	0.007	0.857	0.005	0.840	0.005	ANOVA	0.116	2.20	No
α Diversity		2.407	0.062	2.805	0.088	2.884	0.091	ANOVA	< 0.0005	9.60	Start v Middle, Start v End
γ Diversity		3.235	0.040	3.829	0.068	3.829	0.053	ANOVA	< 0.0005	14.70	Start v Middle, Start v End
β Diversity		0.828	0.794	1.025	0.059	0.945	0.077	ANOVA	0.397	0.93	No
Environmental variables											
Caulophacus debris		0.457	0.110	1.428	0.317	0.915	0.140	K-W, M-W	< 0.0005	17.99	Start v Middle, Start v End
Bathycrinus stalks		1.475	0.118	1.635	0.138	2.298	0.151	ANOVA	< 0.0005	10.41	Start v End, Middle v End
Pourtalesia test		0.077	0.023	0.495	0.256	0.271	0.064	K-W, M-W	0.008	9.64	Start v Middle, Start v End
Burrows		0.311	0.064	0.099	0.036	0.037	0.015	K-W, M-W	< 0.0005	21.65	Start v Middle, Start v End
Lebensspuren		13.724	0.191	16.282	0.377	16.359	0.307	K-W, M-W	< 0.0005	41.20	Start v Middle, Start v End
(Drop) stones		0.082	0.025	0.120	0.035	0.136	0.038	ANOVA	0.492	0.71	No
Anthropogenic litter				0.007	0.007			ANOVA	0.346	1.07	No
Shells		0.865	0.099	0.986	0.117	0.791	0.111	ANOVA	0.450	0.80	No
Pebbles		1.960	0.295	21.024	2.825	28.759	2.384	K-W, M-W	< 0.0005	78.13	Start v Middle, Start v End, Middle v End
Bone		0.071	0.023	0.208	0.046	0.298	0.052	K-W, M-W	< 0.001	15.18	Start v Middle, Start v End

(FT) feeding type (P/S; predator/scavenger, DF; deposit feeder, SF; suspension feeder, n.d.; not defined)
(SE) standard error; f or χ^2; test statistics of ANOVA or Kruskal-Wallis tests.
* indicates taxa/morphotype used for statistical analysis tests.

between the start and middle images and with the middle and end images occupying the same space.

The start section, however, does show a significantly lower α (F=9.60, df=2) and γ (F=14.70, df=2) diversity, whilst showing no significant difference in β diversity (Table 6). The overall α/β diversity contributions to overall γ diversity were 74.40/25.60%, 73.26/26.74% and 75.32/24.68% in the start, middle and end sections, respectively.

Similarly, there was no significant difference in community composition at S3 (Global R=0.089, p=0.001) (Table 7). Similarly, there were no significant differences in overall megafaunal abundance and the abundance of different trophic groups at the three transect sections. The overall α/β diversity contributions to overall γ diversity were 73.29/26.71%, 80.02/19.98% and 76.13/24.87% in the start, middle and end section, respectively. The comparison of the eight biogenic habitat features recorded indicate no dissimilarity (ANOSIM; Global R=0.121, p=0.001) (Table 8).

4. Discussion

Our study is one of the few to address local and regional-scale differences in deep-sea megafauna. It is also the first time that the megafaunal community at stations N3 and S3 of the HAUSGARTEN observatory has been described, which shows taxonomic overlap with HG-IV (Soltwedel et al., 2009; Bergmann et al., 2011). While the species inventory at all three stations was similar, differences in their relative proportions explain the variability observed.

Overall, the taxonomic resolution in this study was high, despite a number of morphotypes. This is primarily due to the extensive previous work at HAUSGARTEN conducted at HG-IV (Bergmann et al., 2009, 2011) and the other stations (Bergmann, unpubl.), which enabled ground-truthing. Certain taxa are more difficult to address with photographic methods compared to invasive methods (e.g. actinarians), however further sampling work at HAUSGARTEN continues to address this. Spatial variability of key species over whole transects can also be studied using machine-learning algorithms (Schoening et al., 2012).

Whilst sites were selected at approximately 2500 m depth based on data from the General Bathymetric Chart of the Oceans (GEBCO), the depths of transects in this study varied, with a difference of 437 m measured at the deepest point (2788 m-N3) to the shallowest (2351 m-S3). Whilst depth is a proven factor in shaping megafaunal communities at HAUSGARTEN (Soltwedel et al., 2009) and cannot be disregarded completely, here we suggest that it is not one of the key contributors to the variation observed between the sites. This is due to the depths studied being accessible to all of the statistically significant species based on known depth ranges (e.g. *Kolga hyalina*: 2030-3413 m+). There was also variation in depth within each transect: N3-125 m, HG-IV-232 m and S3-15 m. Again we suggest that potential variation seen within transect is not a result of the depth difference alone, for the same reason.

4.1. Variations in benthic megafaunal composition at a regional scale

Our results show that there are strong dissimilarities in the benthic megafaunal communities at N3, HG-IV and S3 in 2011 that increases with distance between station, with N3 and S3 showing a completely different community structure. Large dissimilarity was also discovered between N3 and HG-IV and moderate dissimilarity between HG-IV and S3.

The overall megafaunal densities at HG-IV are much lower compared with N3 and S3. While other environmental data did not sufficiently explain this variability, soluble protein, an indicator of the amount of detrital matter reaching the seafloor, was significantly lower. Whilst HG-IV having the lowest concentrations is to be expected because the lower megafaunal densities observed, the inverse of what is expected between N3 and S3 is surprising. One possible explanation is that in this typically food-limited environment the detrital material reaching the seafloor had already been substantially reworked by the entire benthic community. Bett et al. (2001) showed that despite a considerable influx of organic material at the Porcupine Abyssal Plain (PAP) during the "*Amperima* event" (1996–1998; Billett et al., 2001), there was very little evidence of the influx on the seafloor due to rapid reworking of the material by the larger deposit-feeding holothurian, *Amperima rosea* and the ophiuroid, *Ophiocten hastatum*. With increased deposit feeder abundance the area of the seafloor, which had previously taken 2.5 years to track over, now only took the megafauna six weeks to track over and rework the available food sources. Combining this with the findings by Billett et al. (2010), who showed that abyssal ecosystems can change radically over periods of <6 months at PAP with an order of magnitude changes in densities of invertebrate megafauna, which is also mirrored in the meiofauna (Gooday et al., 2009; Kalogeropoulou et al., 2010) and macrofaunal polychaetes (Soto et al., 2010), may indicate that megafaunal communities are potentially more dynamic than previously thought (Ruhl and Smith, 2004; Ruhl et al., 2008; FitzGeorge-Balfour et al., 2010). Megafaunal densities at HG-IV were observed to be similar to those seen in 2002 and 2011, but greater than 2004 and 2007 (Bergmann et al., 2011; Müller et al., 2015).

Two studies on macrobenthic (Vedenin et al., subm.) and bacterial communities (Jacob et al., 2013) along the latitudinal gradient of HAUSGARTEN reported no significant differences in the community composition from station N3 to station S3. This is interesting for two reasons: (1) the factors causing differences in megafaunal communities appear not to affect the smaller sediment-inhabiting biota. (2) This indicates that the spatial scales at work differ for the three size groups. Spatial patterns of macrofauna and bacteria, which could serve as food or change biogeochemical sediment properties, appear not to affect megafaunal community composition.

The species that caused the greatest dissimilarity between our stations was the sea cucumber, *Kolga hyalina*, which had previously been reported at lower densities HG-IV (Bergmann et al., 2011). Interestingly, however, densities were 40 times higher at N3, whereas it was completely absent from S3. A potential reason for the high *Kolga* abundance at N3 could be higher ice concentrations and the subsequent melting and release of associated particulate organic matter. Gutt (1995) showed that the ice algae *Melosira arctica* contributes considerably to algal abundance at the subsurface of the sea ice in a nearby Arctic region and Boetius et al. (2013) demonstrated the potential value of *M. arctica* as a food source for *K. hyalina,* indicating a direct link between primary production at the surface and deep seafloor communities. While it may be premature to label our findings as a potential *Kolga* event, the phenomenon has been documented on other occasions, in which deep-sea holothurians reproduce very successfully after above-average food supply and form very high local aggregations, e.g. *Elpidia glacialis* at Larsen A and B in Antarctica (Gutt et al., 2011), *Amperima rosea* (Billett et al., 2001) and four separate

Table 7
Mean densities (ind. m^{-2}) of megafaunal taxa/morphotypes, biogenic habitat features and diversity indices recorded from different sections of the photographic transect taken at HAUSGARTEN station S3.

Taxon	FT	Start mean	±SE	Middle mean	±SE	End mean	±SE	Test used	*p*	*f* or χ^2	Significant difference
Porifera											
*Caulophacus arcticus**	SF	0.008	0.008	0.030	0.015	0.013	0.009	K-W, M-W	0.413	1.77	No
Cladorhiza cf. *gelida**	SF	0.060	0.027	0.045	0.017	0.116	0.033	K-W, M-W	0.252	2.76	No
Small round sponge	SF	6.635	0.336	7.026	0.266	5.520	0.266	ANOVA	0.001	8.14	Middle v End
Cnidaria											
Purple actinarian*	SF	0.313	0.072	0.275	0.046	0.157	0.030	K-W, M-W	0.144	3.88	No
cf. *Bathyphellia margaritacea**	SF	1.557	0.137	2.050	0.142	2.272	0.168	ANOVA	0.007	5.22	Start v End
*Gersemia fruticosa**	SF	0.613	0.092	0.714	0.084	0.885	0.100	ANOVA	0.124	2.13	No
Hormathiidae*	SF	0.136	0.054	0.567	0.170	0.546	0.108	K-W, M-W	0.001	13.09	Start v Middle, Start v End
White long-tentacled actinarian*	SF	0.353	0.079	0.415	0.080	0.592	0.095	ANOVA	0.135	2.05	No
Ceriantharia	SF	0.105	0.060					ANOVA	0.020	4.09	No (Bonferroni)
Actinaria	SF	0.011	0.011					ANOVA	0.267	1.34	No
Annelida											
*Byglides groenlandicus**	P/S	0.106	0.046	0.097	0.030	0.058	0.019	ANOVA	0.704	0.70	No
Mollusca											
Mohnia spp.*	P/S	0.750	0.081	0.372	0.056	0.583	0.064	ANOVA	0.001	7.77	Start v Middle
Pycnogonida											
*Ascorhynchus abyssi**	P/S	0.254	0.055	0.376	0.073	0.340	0.048	ANOVA	0.382	0.97	No
Crustacea											
*Neohela lamia**	DF	0.128	0.034	0.362	0.054	0.282	0.062	K-W, M-W	0.005	10.44	Start v Middle
*Saduria megalura**	n.d.	0.009	0.009	0.014	0.010	0.027	0.013	K-W, M-W	0.497	1.40	No
Bythocaris spp.*	P/S					0.070	0.024	ANOVA	0.001	7.17	Start v End, Middle v End
Isopoda	DF	4.864	0.383	4.598	0.248	4.758	0.225	ANOVA	0.802	0.22	No
Birsteiniamysis inermis	n.d.	0.067	0.027	0.036	0.015	0.071	0.021	ANOVA	0.424	0.86	No
Halirages cainae	n.d.	0.040	0.019	0.021	0.012	0.008	0.008	K-W, M-W	0.224	2.99	No
Echinodermata											
*Elpidia heckeri**	DF	0.801	0.106	0.958	0.106	0.727	0.076	ANOVA	0.199	1.64	No
*Bathycrinus carpenterii**	SF	0.757	0.085	0.790	0.082	0.937	0.085	ANOVA	0.271	1.32	No
*Hymenaster pellucidus**	P/S			0.007	0.007			ANOVA	0.397	0.93	No
*Pourtalesia jeffreysi**	DF	0.086	0.026	0.254	0.043	0.252	0.037	K-W, M-W	0.002	12.70	Start v Middle, Start v End
Pisces											
*Lycodes frigidus**	P/S	0.008	0.008	0.007	0.007			ANOVA	0.543	0.61	No
Feeding types											
Predator/scavengers		1.119	0.086	0.859	0.096	1.051	0.099	ANOVA	0.154	1.91	No
Suspension feeders		10.548	0.392	11.910	0.466	11.037	0.485	ANOVA	0.126	2.11	No
Deposit feeders		5.879	0.394	6.171	0.281	6.018	0.241	ANOVA	0.799	0.22	No
Not defined		0.116	0.039	0.071	0.024	0.105	0.026	ANOVA	0.519	0.66	No
Overall densities		17.662	0.715	19.012	0.660	18.212	0.649	ANOVA	0.388	0.96	No
Diversity indices											
Shannon-Wiener ***H***		1.730	0.035	1.804	0.031	1.902	0.025	ANOVA	< 0.0005	8.33	Start v End
Pilou's evenness ***J***		0.750	0.011	0.751	0.008	0.785	0.007	ANOVA	0.005	5.70	Start v End, Middle v End
α Diversity		2.811	0.125	3.188	0.113	3.291	0.097	ANOVA	0.010	4.78	Start v End
γ Diversity		3.835	0.092	3.984	0.079	4.323	0.080	ANOVA	0.227	1.50	No
β Diversity		1.023	0.100	0.796	0.081	1.031	0.081	ANOVA	0.094	2.42	No
Environmental variables											
Caulophacus debris		0.104	0.034	0.179	0.053	0.159	0.034	K-W, M-W	0.316	2.30	No
Bathycrinus stalks		0.499	0.064	0.389	0.061	0.442	0.079	ANOVA	0.575	0.56	No
Pourtalesia test		0.194	0.052	0.182	0.057	0.111	0.038	ANOVA	0.427	0.86	No
Burrows		1.115	0.136	1.931	0.176	1.840	0.168	ANOVA	0.002	6.49	Start v Middle, Start v End
Lebensspuren		13.556	0.585	16.634	0.422	17.375	0.392	ANOVA	< 0.0005	17.97	Start v Middle, Start v End
(Drop) stones		0.094	0.028	0.147	0.045	0.109	0.033	K-W, M-W	0.929	0.15	No
Shells		0.053	0.035	0.108	0.023	0.027	0.013	K-W, M-W	0.004	11.29	Start v Middle, Start v End
Pebbles		2.060	0.266	0.772	0.089	0.573	0.078	K-W, M-W	< 0.0005	36.24	Start v Middle, Start v End

(FT) feeding type (P/S; predator/scavenger, DF; deposit feeder, SF; suspension feeder, n.d.; not defined)

(SE) standard error; f or χ^2; test statistics of ANOVA or Kruskal-Wallis tests.
* indicates taxa/morphotype used for statistical analysis tests.

Table 8
ANOSIM results of biogenic habitat feature composition taken from photographic transects at HAUSGARTEN stations N3, HG-IV and S3.

Sections compared	N3	HG-IV	S3
Start v Middle	0.203	0.133	0.150
Start v End	0.300	0.440	0.238
Middle v End	0.029	0.360	0.008

species including *Scotoplanes globosa* at Station M (Kuhnz et al., 2014). Preliminary results of our megafaunal time series indicate increased *Kolga* densities at N3 in 2007 and 2011 compared with 2004 (Taylor, 2012; Taylor, unpubl.). Despite increased numbers of *Kolga* and deposit feeders in general at N3 and S3, both stations still mirror HG-IV in being a community with a greater quantity of suspension feeders (Soltwedel et al., 2009; Bergmann et al., 2011). N3 has, however, a significantly higher number of predator/scavengers, due to higher densities of the gastropod *Mohnia* spp. With higher abundances and greater trophic diversity being correlated with the health and maturity of an ecosystem (Sandin and Sala, 2012) it could be argued that N3 is the most established community, which is supported by higher diversity indices. When looking at the α, β and γ richness diversities we can see that HG-IV is characterised by the greatest γ diversity, i.e. the greatest overall species richness per m^{-2}. HG-IV also shows the greatest species turnover, β diversity, but, significantly, the lowest α diversity, i.e. established community. This means that HG-IV is characterised by the greatest species heterogeneity, but also the greatest proportion of species turnover, indicating a less established community.

The biogenic habitat features did not show a significant variation in composition and it is unlikely that they have an as strong effect on the megafaunal compositions seen in this study as food influx to the seafloor does. The observed biogenic habitat features are likely defined by the biota rather than defining the biota, especially those specifically related to particular taxa such as *Caulophacus* debris, *Bathycrinus* stalks and *Pourtalesia jeffreysii* tests. However, the result of higher pebble quantities at N3, likely released from the sea–ice above during melt events, does potentially allow for a unique, and quicker, route of food availability into the ecosystem, thus having a direct effect on the local ecosystem, such as the local meiofauna (Hasemann et al., 2013) and therefore local megafauna also.

4.2. Variations in benthic megafaunal composition at a local scale at HG-IV.

Significant local-scale variation was only found at HG-IV with the start section standing out to such an extent that the two transect ends can be considered separate communities. Whilst low to moderate variability in abiotic factors may account for a certain amount of this variance, it is not enough to begin to explain it fully.

At HG-IV, there are no differences in overall megafaunal abundance, which is surprising given the high variability in community structure between transect sections. While this suggests that food availability is similar across the transect, we do see a significant decrease in predators/scavengers and significant increase in suspension feeders and deposit feeders towards the shallower parts, implying that the type of food on offer rather than the availability is causing a greater effect on the community composition or local differences in the bottom current regime.

The HG-IV transect runs along a slope spanning over 200 m (Fig. 9). This is a relatively large range and the associated slope effects are likely to be some of the main drivers in the two completely differing communities at the beginning and end of this transect. For example whilst this depth range is generally inhabitable to *Kolga hyalina* (Billett, 1991) it may not be due to physical properties such as porosity/type of substrata or varying currents or species interactions. Our findings here are in line with Jones et al. (2013) who also show decreasing deposit feeder numbers and increasing suspension feeder numbers with increasing slope. The finding of a community shift within HG-IV due to these reasons has also been seen along the entirety of the bathymetric transect, within smaller depth ranges, by Soltwedel et al. (2009). Because of this, potentially, only the start of this transect should be used for future latitudinal studies or potentially only look at the northern and southern stations for latitudinal studies, whilst continuing to study HG-IV in its own right.

5. Conclusion

In reference to our scientific aims we have shown that megafaunal density varies greatly along a latitudinal gradient, with highest densities at the northernmost station, followed by the southernmost station and the central HG-IV station. We also observed significantly different species compositions at each station leading to variations in trophic structure and species diversity

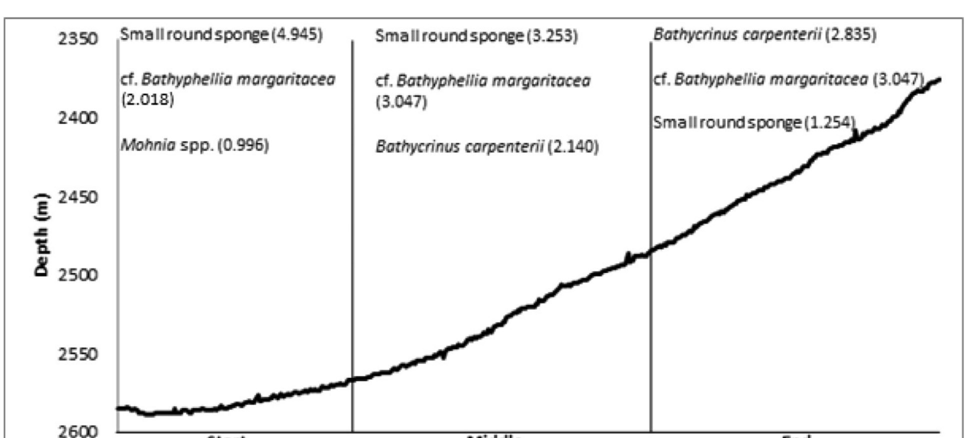

Fig. 9. Plot of the depth along the photographic transect taken at HAUSGARTEN HG-IV showing the three most abundant taxa in each section (ind. m^{-2}).

measures. Potential explanations for these variations include significantly different protein availability, as well as potential increases in food input at N3 and S3. The latter were not captured by our measurements of environmental variables possibly because of fast reworking of sediments by local deposit feeders and infauna. Also, ice concentration above a station is significant and has a direct impact on the type of food that reaches the benthic community. The phytodetrital matter in the case of *Melosira arctica,* may in turn also shape the benthic community composition, particularly on the deep-sea holothurian, *Kolga hyalina*. While there were no-moderate local-scale differences at stations N3 and S3a complete community shift was found within a distance of two nautical miles at HG-IV. This was most likely driven by the slope or unidentified slope-driven factors at this transect.

Acknowledgements

We thank the officers and crew of *R/V Polarstern* for their assistance at sea during expedition ARK-XXV/2 to HAUSGARTEN and I. Schewe for supervising OFOS transects and multiple corer deployments. C. Hasemann took care of sediment analyses. The following taxonomic experts are thanked for their assistance in identification of specimens from images: A. Vedenin, N. Budaeva (P.P. Shirshov Institute of Oceanology), M. Wicksten (Texas A&M University), D. Janussen (Senckenberg Museum of Natural History). T. Schoening (Universität Bielefeld) provided user support with BIIGLE, which was partly funded by the Helmholtz Alliance ROBEX as was MB. This study contributes to the tasks of the Helmholtz-funded programme FRAM (Frontiers in Arctic Marine Research). The suggestions of two anonymous reviewers improved an earlier version of the manuscript. JT was funded by a DAAD PhD scholarship. This publication is Eprint ID 38239 of the Alfred-Wegener-Institut Helmholtz-Zentrum für Polar- und Meeresforschung.

References

Bauerfeind, E., Nöthig, E.-M., Beszczynska, A., Fahl, K., Kaleschke, L., Kreker, K., Klages, M., Soltwedel, T., Lorenzen, C., Wegner, J., 2009. Particle sedimentation patterns in the eastern Fram Strait during 2000–2005: results from the Arctic long-term observatory HAUSGARTEN. Deep-Sea Res. I 56, 1471–1487.
Bergmann, M., Soltwedel, T., Klages, M., 2011. Interannual dynamics of megafaunal assemblages from the Arctic deep-sea observatory, HAUSGARTEN (79°N). Deep-Sea Res. I 58, 711–723.
Bergmann, M., Dannheim, J., Bauerfeind, E., Klages, M., 2009. Trophic relationships along a bathymetric gradient at the deep-sea observatory HAUSGARTEN. Deep-Sea Res. I 56, 408–424.
Bergmann, M., Klages, M., 2012. Increase of litter at the Arctic deep-sea observatory HAUSGARTEN. Mar. Pollut. Bull. 64, 2734–2741.
Beszczynska-MÖller, A., Fahrbach, E., Schauer, U., Hansen, E., 2012. Variability in Atlantic water temperature and transport at the entrance to the Arctic Ocean, 1997–2010. ICES J. Mar. Sci. 69, 852–863.
Bett, B.J., Malzone, M.G., Narayanaswamy, B.E., Wigham, B.D., 2001. Temporal variability in phytodetritus and megabenthic activity at the seabed in the deep Northeast Atlantic. Prog. Ocean. 50, 349–368.
Billett, D.S.M., 1991. Deep-Sea Holothurians. Ocean. Mar. Biol. 29, 259–317.
Billett, D.S.M., Bett, B.J., Rice, A.L., Thurston, M.H., Galéron, J., Sibuet, M., Wolff, G.A., 2001. Long-term change in the megabenthos of the Porcupine Abyssal Plain (NE Atlantic). Prog. Ocean. 50, 325–348.
Billett, D.S.M., Bett, B.J., Reid, W.D.K., Boorman, B., Priede, I.G., 2010. Long-term change in the abyssal NE Atlantic: the '*Amperima* Event' revisited. Deep-Sea Res. II 57, 1406–1417.
Boetius, A., Albrecht, S., Bakker, K., Bienhold, C., Felden, J., Fernandez-Mendez, M., Hendricks, S., Katlein, C., Lalande, C., Krumpen, T., Nicolaus, M., Peeken, I., Rabe, B., Rogacheva, A., Rybakova, E., Somavilla, R., Wenzhöfer, F., 2013. Export of Algal Biomass from Melting Arctic Sea Ice. Science 339, 1430–1432.
Buhl-Mortensen, L., Tandberg, A.H.S., Buhl-Mortensen, P., Gates, A.R., 2015. Behaviour and habitat of *Neohela monstrosa* (Boeck, 1861) (Amphipoda: Corophiida) in Norwegian Sea deep water. J. Nat. Hist. 50, 323–337. http://dx.doi.org/10.1080/00222933.2015.1062152.
Buhl-Mortensen, L., Vanreusel, A., Gooday, A.J., Levin, L.A., Priede, I.G., Buhl- Mortensen, P., Gheerardyn, H., King, N.J., Raes, M., 2010. Biological structures as a source of habitat heterogeneity and biodiversity on the deep ocean margins. Mar. Ecol. 31, 21–50.
Carmack, E., Wassmann, P., 2006. Food webs and physical-biological coupling on pan-Arctic shelves: unifying concepts and comprehensive perspectives. Prog. Ocean. 71, 446–477.
Clarke, K.R., Gorley, R.N., 2006. Primer v6: User Manual/Tutorial. PRIMER-E, Plymouth, p. 190.
Crist, T.O., Veech, J.A., 2006. Additive partitioning of rarefaction curves and species-area relationships: unifying alpha-, beta- and gamma-diversity with sample size and habitat area. Ecol. Lett. 9, 923–932. http://dx.doi.org/10.1111/j.1461-0248.2006.00941.x.
Ezraty, R., Girard-Ardhuin, F., Piollé, J.F., Kaleschke, L., Heygster, G., 2007. Arctic and Antarctic Sea Ice Concentration and Arctic Sea Ice Drift Estimated from Special Sensor Microwave Data. Département d'Océanographie Physique et Spatiale, IFREMER, Brest, France and University of Bremen Germany, 2.1edn. /urlprefix/url⟨ftp://ftp.ifremer.fr/ifremer/cersat/products/gridded/psi-drift/documentation/ssmi.pdf⟩.
Fahrbach, E., Meincke, J., Osterhus, S., Rohardt, G., Schauer, U., Tverberg, V., Verduin, J., 2001. Direct measurements of volume transports through Fram Strait. Polar Res. 20, 217–224.
FitzGeorge-Balfour, T., Billett, D.S.M., Wolff, G.A., Thompson, A., Tyler, P.A., 2010. Phytopigments as biomarkers of selectivity in abyssal holothurians; interspecific differences in response to a changing food supply. Deep-Sea Res. II 57, 1418–1428.
Forest, A., Wassmann, P., Slagstad, D., Bauerfeind, E., Nöthig, E.-M., Klages, M., 2010. Relationships between primary production and vertical particle export at the Atlantic-Arctic boundary (Fram Strait, HAUSGARTEN). Polar Biol. 33, 1733–1746.
Gooday, A.J., Levin, L.A., Aranda da Silva, A., Bett, B.J., Cowie, G.L., Dissard, D., Gage, J. D., Hughes, D.J., Jeffreys, R., Lamont, P.A., Larkin, K.E., Murty, S.J., Schumacher, S., Whitcraft, C., Woulds, C., 2009. Faunal responses to oxygen gradients on the Pakistan margin: A comparison of foraminiferans, macrofauna and megafauna. Deep. Sea Res. II 56, 488–502.
Górska, B., Grzelak, K., Kotwicki, L., Hasemann, C., Schewe, I., Soltwedel, T., Wlodarska-Kowalczuk, M., 2014. Bathymetric variations in vertical distribution patterns of meiofauna in the surface sediments of the deep Arctic ocean (HAUSGARTEN, Fram Strait. Deep-Sea Res. I 91, 36–49.
Grassle, J.F., Sanders, H.L., Hessler, R.R., Rowe, G.T., McLellan, T., 1975. Pattern and zonation: a study of the bathyal megafauna using the research submersible Alvin. Deep-Sea Res. Ocean. Abstr. 22, 457–462.
Grassle, J.F., Maciolek, N.J., 1992. Deep-sea species richness: regional and local diversity estimates from quantitative bottom samples. Am. Nat. 139, 313–341.
Gutt, J., 1995. The occurrence of sub-ice algal aggregations off northeast Greenland. Polar Biol. 15, 247–252.
Gutt, J., Barratt, I., Domack, E., d'Udekem d'Acoz, C., Dimmler, W., Grémare, A., Heilmayer, O., Isla, E., Janussen, D., Jorgensen, E., Kock, K.-H., Lehnert, L.S., López-Gonzáles, P., Langner, S., Linse, K., Manjón-Cabeza, M.E., Meißner, M., Montiel, A., Raes, M., Robert, H., Rose, A., Sañé Schepisi, E., Saucède, T., Scheidat, M., Schenke, H.-W., Seiler, J., Smith, C., 2011. Biodiversity change after climate-induced ice-shelf collapse in the Antarctic. Deep-Sea Res. II 58, 74–83.
Hasemann, C., Soltwedel, T., 2011. Small-scale heterogeneity in deep-sea nematode communities around biogenic structures. PLoS One 6, e29152.
Hasemann, C., Bergmann, M., Kanzog, C., Lochthofen, N., Sauter, E., Schewe, I., Soltwedel, T., 2013. Effects of dropstone induced habitat heterogeneity on Arctic deep-sea benthos with special reference to nematode communities. Mar. Biol. Res. 9, 276–292.
Hirche, H.-J., Kosobokova, K., 2007. Distribution of *Calanus finmarchicus* in the northern North Atlantic and Arctic Ocean-Expatriation and potential colonization. Deep-Sea Res. II 54, 2729–2747.
Hop, H., Falk-Petersen, S., Svendsen, H., Kwasniewski, S., Pavlov, V., Pavlova, O., Søreide, J.E., 2006. Physical and biological characteristics of the pelagic system across Fram Strait to Kongsfjorden. Prog. Ocean. 71, 182–231.
Hoste, E., Vanhove, S., Schewe, I., Soltwedel, T., Vanreusel, A., 2007. Spatial and temporal variations in deep-sea meiofauna assemblages in the Marginal Ice Zone of the Arctic Ocean. Deep-Sea Res. 54, 109–129.
Jacob, M., Soltwedel, T., Boetius, A., Ramette, A., 2013. Biogeography of Deep-Sea Benthic Bacteria at Regional Scale (LTER HAUSGARTEN, Fram Strait, Arctic. PLoS One 8, e72779.
Jones, C.G., Lawton, J.H., Shachak, M., 1994. Organisms as ecosystem engineers. OIKOS 69, 373–386.
Jones, D.O.B., Mrabure, C.O., Gates, A.R., 2013. Changes in deep-water epibenthic megafaunal assemblages in relation to seabed slope on the Nigerian margin. Deep-Sea Res. I 78, 49–57.
Kalogeropoulou, V., Bett, B.J., Gooday, A.J., Lampadariou, N., Arbizu, P.M., Vanreusel, A., 2010. Temporal changes (1989–1999) in deep-sea metazoan meiofaunal assemblages on the Porcupine Abyssal Plain, NE Atlantic. Deep-Sea Res. II 57, 1383–1395.
Kauker, F., Kaminski, T., Karcher, M., Giering, R., Gerdes, R., Vossbeck, M., 2009. Adjoint analysis of the 2007 all time Arctic sea–ice minimum. Geophys. Res. Lett. 36, L03707.
Kuhnz, L.A., Ruhl, H.A., Huffard, C.L., Smith Jr., K.L., 2014. Rapid changes and long-term cycles in the benthic megafaunal community observed over 24 years in the abyssal northeast Pacific. Prog. Ocean. 124, 1–11.
Meyer, K.S., Bergmann, M., Soltwedel, T., 2013. Interannual variation in the epibenthic megafauna at the shallowest station of the HAUSGARTEN observatory (79°N, 6°E). Biogeosciences 10, 3479–3492.
Meyer, K.S., Soltwedel, T., Bergmann, M., 2014. High biodiversity on a deep-water reef in the Eastern Fram Strait. PLoS One 9, e105424.
Müller, F., Bergmann, M., Dannowski, R., Dippner, J.W., Gnauck, A., Haase, P., Jochimsen, M.C., Kasprzak, P., Kröncke, I., Kümmerlin, R., Küster, M., Lischeid, G.,

Meesenburg, S., Merz, C., Millat, G., Müller, J., Padisák, J., Schimming, C.G., Schubert, H., Schult, M., Selmeczy, G., Shatwell, T., Stoll, S., Schwabe, M., Soltwedel, T., Straile, D., 2015. Assessing resilience in long-term ecological data sets. Ecol. Indic. . http://dx.doi.org/10.1016/j.ecolind.2015.10.066, in press

Ontrup, J., Ehnert, N., Bergmann, M., Nattkemper, T.W., 2009. Biigle – Web 2.0 enabled labelling and exploring of images from the Arctic deep-sea observatory HAUSGARTEN, OCEANS 2009 – EUROPE. 2009 doi: 10.1109/OCEANSE.2009.5278332.

Pantke, C., 2014. Artenzusammensetzung arktischer Tiefseeschwämme (Porifera) im HAUSGARTEN vor Spitzbergen. Philipps-Universität Marburg, Marburg.

Quéric, N.-V., Soltwedel, T., 2007. Impact of small-scale biogenic sediment structures on bacterial distribution and activity in Arctic deep-sea sediments. Mar. Ecol. 28, 66–74.

Rex, M.A., 1981. Community structure in the deep-sea benthos. Annu. Rev. Ecol. Syst. 12, 331–353.

Rex, M.A., Stuart, C.T., Hessler, R.R., Allen, J.A., Sanders, H.L., Wilson, G.D.F., 1993. Global-scale latitudinal patterns of species diversity in the deep-sea benthos. Nature 365, 636–639.

Ruhl, H.A., 2007. Abundance and size distribution dynamics of abyssal epibenthic megafauna in the northeast Pacific. Ecology 88, 1250–1262.

Ruhl, H.A., Smith Jr., K.L., 2004. Shifts in deep-sea community structure linked to climate and food supply. Science 305, 513–515.

Ruhl, H.A., Ellena, J.A., Smith, K.L., 2008. Connections between climate, food limitation, and carbon cycling in abyssal sediment communities. Proc. Natl. Acad. Sci. 105, 17006–17011.

Sandin, S.A., Sala, E., 2012. Using successional theory to measure marine ecosystem health. Evol. Ecol. 26, 435–448.

Schewe, I., Soltwedel, T., 2003. Benthic response to ice-edge induced particle flux in the Arctic Ocean. Polar Biol. 26, 610–620.

Schoening, T., Bergmann, M., Ontrup, J., Taylor, J., Dannheim, J., Gutt, J., Purser, A., Nattkemper, T.W., 2012. Semi-automated image analysis for the assessment of megafaunal densities at the Arctic deep-sea Observatory HAUSGARTEN. PLoS One 7, e38179.

Schoening, T., Kuhn, T., Bergmann, M., Nattkemper, T.W., 2015. Delphi-an iteratively learning laser point detection. Front. Mar. Sci. 2 (2015), 00020.

Soto, E.H., Paterson, G.L.J., Billett, D.S.M., Hawkins, L.E., Galeron, J., Sibuet, M., 2010. Temporal variability in polychaete assemblages of the abyssal NE Atlantic Ocean. Deep-Sea Res. II 57, 1396–1405.

Smith, C.R., De Leo, F.C., Bernardino, A.F., Sweetman, A.K., Arbizu, P.M., 2008. Abyssal food limitation, ecosystem structure and climate change. Trends Ecol. Evol. 9, 518–528.

Smith, K.L., Ruhl, H.A., Bett, B.J., Billett, D.S.M., Lampitt, R.S., Kaufmann, R.S., 2009. Climate, carbon cycling, and deep-ocean ecosystems. Proc. Natl. Acad. Sci. 106, 19211–19218.

Soltwedel, T., Bauerfeind, E., Bergmann, M., Budaeva, N., Hoste, E., Jaeckisch, N., von Juterzenka, K., Matthiessen, J., Mokievsky, V., Nöthig, E.-M., Quéric, N.-V., Sablotny, M., Sauter, E., Schewe, I., Urban-Malinga, B., Wegner, J., Wlodarska-Kowalczuk, M., Klages, M., 2005. HAUSGARTEN-multidisciplinary investigations at a deep-sea long-term observatory in the Arctic Ocean. Oceanography 18, 46–61.

Soltwedel, T., Jaeckisch, N., Ritter, N., Hasemann, C., Bergmann, M., Klages, M., 2009. Bathymetric patterns of megafaunal assemblages from the arctic deep- sea observatory HAUSGARTEN. Deep-Sea Res. I 56, 1856–1872.

Soltwedel, T., Vopel, K., 2001. Bacterial abundance and biomass in response to organism-generated habitat heterogeneity in deep-sea sediments. Mar. Ecol. Prog. Ser. 219, 291–298.

Spreen, G., Kaleschke, L., Heygster, G., 2008. Sea Ice Remote Sensing Using AMSR-E 89 GHz Channels. J. Geophys. Res. 113, 1–14.

Sswat, M., Gulliksen, B., Menn, I., Sweetman, A.K., Piepenburg, D., 2015. Distribution and composition of the epibenthic megafauna north of Svalbard (Arctic). Polar Biol. 38, 861–877.

Thiel, H., 1978. Benthos in upwelling regions. In: Boje, R., Tomczak, M. (Eds.), Upwelling ecosystems. Springer, Berlin, pp. 124–138.

Taylor, J., 2012. A Study and Comparison of Species Composition and the Influencing Abiotic Factors of the Benthic Ecosystems at HAUSGARTEN IV, N3 and S3 in 2004 and 2007. University of Glasgow, UK.

Vedenin, A., Budaeva, N., Mokievsky V.O., Pantke, C., Soltwedel, T., Gebruk, A., 2015. Spatial distribution patterns in macrobenthos along a latitudinal transect at the deep-sea observatory HAUSGARTEN (in submission).

Veech, J.A., Crist, T.O., 2010. Diversity partitioning without statistical independence of alpha and beta. Ecology 91, 1964–1969.

von Appen, W.-J., Schauer, U., Somavilla Cabrillo, R., Bauerfeind, E., Beszczynska-Möller, A., 2015. Exchange of warming deep waters across Fram Strait. Deep-Sea Res. I 103, 86–100.

Wassmann, P., Slagstad, D., Ellingsen, I., 2010. Primary production and climatic variability in the European sector of the Arctic Ocean prior to 2007: preliminary results. Polar Biol. 12, 1641–1650.

Wedding, L.M., Friedlander, A.M., Kittinger, J.N., Watling, L., Gaines, S.D., Bennett, M., Hardy, S.M., Smith, C.R., 2013. From principles to practice: a spatial approach to systematic conservation planning in the deep sea. Proc. R. Soc. Lond. B 280, 20131684.

Whitman, J.D., Etter, R.J., Smith, F., 2004. The relationship between regional and local species diversity in marine benthic communities: a global perspective. Proc. Natl. Acad. Sci. USA 101, 15664–15669.

Whittaker, R.H., 1960. Vegetation of the Siskiyou mountains. 30. Ecological Monographs, Oregon and California, pp. 280–338.

Wlodarska-Kowalczuk, M., Kendall, M.A., Weslawski, J.M., Klages, M., Soltwedel, T., 2004. Depth gradients of benthic standing stock and diversity on the continental margin at a high-latitude ice-free site (off Spitsbergen, 79°N). Deep. Sea Res. I 51 (12), 1903–1914.

Zhang, Q., Hou, X., Li, F.Y., Niu, J., Zhou, Y., Ding, Y., Zhao, L.Q., Li, X., Ma, W.J., Kang, S., 2014. Alpha, beta and gamma diversity differ in response to precipitation in the Inner Mongolia Grassland. PLoS One 9, e93518. http://dx.doi.org/10.1371/journal.pone.0093518.